

Supporting Information For

Probing Adsorption Interactions In Metal-Organic Frameworks Using X-ray Spectroscopy

Walter S. Drisdell¹, Roberta Poloni^{1,2,3,4}, Thomas M. McDonald¹, Jeffrey R. Long^{1,4}, Berend Smit^{2,3}, Jeffrey B. Neaton¹, David Prendergast¹, Jeffrey B. Kortright¹

¹*Materials Sciences Division, Lawrence Berkeley National Laboratory,
Berkeley, California 94720, USA*

²*Department of Chemical and Biomolecular Engineering, University of California,
Berkeley, California 94720-1460, USA*

³*Department of Chemistry, University of California, Berkeley, California 94720-1460, USA*

⁴*Laboratoire de Science et Ingénierie des Matériaux et Procédés (SIMaP), UMR CNRS 5266,
Grenoble-INP, BP 75, 38402 Saint Martin d'Hères Cedex, France*

1. Synthetic Details and Sample Preparation

1.1 Materials:

All reagents were obtained from commercial vendors and used without further purification. UHP-grade (99.999% purity) dinitrogen and helium were used for all adsorption measurements. The Si₃N₄ membranes used are 2mm square and 100nm thick, on a 10mm square silicon frame that is 525 μm thick (Silson).

1.2 Synthesis of bulk Mg-MOF-74 powder:

The metal-organic framework was synthesized, washed repeatedly with DMF and MeOH, and activated at 250 °C for 5 hours as previously reported¹. Nitrogen adsorption at 77 K as shown in Figure S1 (Langmuir surface area 1890 m²/g) confirmed proper activation of the sample. The sample was transferred to a dinitrogen glove box and divided.

1.3 Preparation of DMF ligated Mg-MOF-74 samples:

To ca. 50 mg of activated Mg-MOF-74 powder in a 20 mL scintillation vial, 5 mL of DMF were added. The suspension was filtered, collected, and dispersed in a small amount (ca 0.5 mL) of acetone and sonicated until a homogenous suspension was obtained. Transmission samples were prepared by depositing the suspension on the surface of Si₃N₄ membranes and allowing the solvent to evaporate leaving a coating of powder on the membranes. Samples with deposited metal-organic framework were loaded into the gas cell under ambient air. To remove guest species from the pore, the gas cell was pumped to $<10^{-4}$ Torr, but the samples were not heated to ensure DMF remained coordinated to the Mg²⁺ sites.

1.4 Preparation of activated Mg-MOF-74 samples:

To ca. 50 mg of activated Mg-MOF-74 powder in a 20 mL scintillation vial, 5 mL of MeOH were added. The solid was filtered, collected, and dispersed in a small amount (ca 0.5 mL) of MeOH and sonicated until a homogenous suspension was obtained. Transmission samples were prepared by depositing the suspension on the surface of Si₃N₄ membranes and allowing the solvent to evaporate leaving a coating of powder on the membranes. Samples with deposited metal-organic framework were loaded into a glass evacuation chamber and slowly evacuated of pore guests until a pressure of 50 mTorr was reached. To remove MeOH coordinated to the Mg²⁺ sites, the evacuation chamber was heated to 250 °C for 5 hours with a sand bath. The chamber was cooled to room temperature and slowly refilled with dinitrogen. The samples were transferred from the evacuation chamber to the gas cell in a glove box under a nitrogen purge to ensure that they were not exposed to water vapor before measurement.

1.5 Synthesis of bulk Mg₂(dobpdc) powder:

The metal-organic framework was synthesized as previously reported except DMF was used for the synthesis solvent instead of DEF². After washing with DMF, the sample was divided. An aliquot of ca. 100 mg was activated at 420 °C for 65 min. Nitrogen adsorption at 77 K as shown in Figure S1 (Langmuir surface area 3770 m²/g) confirmed the integrity of the sample. The activated sample was transferred to a dinitrogen glove bag and treated with mmen as reported below in Section 1.2.7.

1.6 Preparation of activated Mg₂(dobpdc) samples:

To ca. 50 mg of DMF solvated Mg₂(dobpdc) powder in a 20 mL scintillation vial, a small amount (ca 0.5 mL) of acetone was added. The vial was sonicated until a homogenous suspension was obtained. Transmission samples were prepared by depositing the suspension on the surface of Si₃N₄ membranes, and allowing the solvent to evaporate leaving a coating of powder on the membranes. Samples with deposited metal-organic framework were loaded into a glass evacuation chamber and slowly evacuated of pore guests until a pressure of 50 mTorr was reached. To remove DMF coordinated to the Mg²⁺ sites, the evacuation chamber was heated to 420 °C for 1 hour with a sand bath. The chamber was cooled to room temperature and slowly refilled with dinitrogen. The samples were transferred from the evacuation chamber to the gas cell in a glove box under a nitrogen purge to ensure that they were not exposed to water vapor before measurement.

1.7 Preparation of mmen ligated Mg₂(dobpdc) samples:

To activated Mg₂(dobpdc) powder in a Micromeritics brand gas adsorption sample tube, 10 mL of anhydrous hexane containing 0.5 mL of *N,N'*-dimethylethylenediamine (mmen) were added. The suspension was sonicated and allowed to sit for an hour. The solid was filtered,

rinsed copiously with dry hexanes, collected, and dispersed in a small amount (ca 0.5 mL) of hexanes and sonicated until a homogenous suspension was obtained. Transmission samples were prepared by depositing the suspension on the surface of Si₃N₄ membranes and allowing the solvent to evaporate leaving a coating of powder on the membranes. Samples with deposited metal-organic framework were loaded into the gas cell under ambient air. To remove guest species from the pore, the gas cell was pumped to a pressure of $<10^{-4}$ Torr, but the samples were not heated to ensure mmen remained coordinated to the Mg sites.

2. NEXAFS Spectra of MgO

To align the energy of the experimental NEXAFS spectra, we collected the NEXAFS spectrum of cubic, single crystal MgO using total electron yield detection, shown in Figure S1. Given the dependence of the NEXAFS spectra of Mg-MOF-74 on the symmetry at the Mg site, we compute the NEXAFS spectra of MgO with and without an apical distortion of one of the octahedral oxygen atoms, to determine if the changing symmetry will have a similar effect on the NEXAFS spectrum of this crystal. The ground state crystal structure was optimized employing SIESTA and using a unit cell of 128 atoms with resulting Mg-O bond length of 2.15 Å. The computed spectrum of octahedral MgO is shown in Figure S1, in very good agreement with our experimental spectrum.

The apical distortion was imposed by lengthening one apical Mg-O distance by 0.5 and 1.0 Å. See the main text for a comparison of the computed NEXAFS spectra with and without distortions. In Figure S2 we report the wavefunction corresponding to the two lowest energy core-excited states for octahedral MgO and MgO with the 0.5 angstrom distortion, from the XCH calculation. We can see that for the MgO structure with an apical distortion, the symmetry of the

spherical lobe at the Mg site is broken and a distorted lobe appears pointing towards the apical distortion. For octahedral MgO, transitions to both states are forbidden by the electric dipole selection rules, but they become XAS active when the apical distortion is imposed. This shows that, like the case of MOF-74 in the presence of adsorbed molecules, the symmetry change at the Mg site could be probed using NEXAFS spectroscopy.

4. Mg₂(dobpdc) Spectra

We also collected spectra of Mg₂(dobpdc) (dobpdc⁴⁻=4,4'-dioxido-3,3'-biphenyldicarboxylate)², an expanded analogue to Mg-MOF-74 with longer organic linkers. Figure S5 shows the full series of spectra for this MOF, taken in vacuum, at CO₂ pressures of 25 Torr, 49 Torr, and 76 Torr, and in vacuum again after the gas was pumped out. These data suffered from time-dependent signal drift which complicates the normalization, preventing a definitive measure of the relative intensities at the main adsorption edge. Spectra are thus normalized to the main peak intensity, and we limit interpretation to the pre-edge region. A pre-edge peak appears for the activated MOF that is suppressed upon CO₂ adsorption. The peak reappears when the gas is pumped out, which is similar to the behavior observed for Mg-MOF-74. For Mg₂(dobpdc), however, this peak is not as pronounced.

This MOF was originally synthesized in order to facilitate chemical functionalization of the Mg sites, specifically with *N,N'*-dimethylethylenediamine (mmen), a double-ended amine that binds CO₂ at very low pressures when appended to the metal centers in the MOF². Figure S6a shows a comparison between the spectra for activated Mg₂(dobpdc), Mg₂(dobpdc) in 76 Torr CO₂, and mmen-Mg₂(dobpdc). While the pre-edge feature is less pronounced for activated Mg₂(dobpdc) than it is for activated Mg-MOF-74, the same suppression of the pre-edge peak is

observed upon adsorption of CO₂. When mmen is appended, the spectrum closely resembles the CO₂ adsorbed case, although a slight redistribution of spectral weight is apparent. Figure S6b shows the computed spectra and transition probabilities for Mg₂(dobpdc), and here some significant disagreements are seen when compared to experiment. Overall, the computed spectra show the same changes seen for Mg-MOF-74. The intensity of the strongest main edge peak is predicted to have an even larger sensitivity to adsorbed species when compared to Mg-MOF-74, which cannot be confirmed from experiment due to the normalization problems. The theory also predicts a blueshift of the main edge absorption onset that is not seen in experiment. With the longer organic linkers in this MOF, thermal effects have a stronger impact on local atomic geometry, and may explain some of the differences between experiment and theory; more detailed studies are needed to test this. In the pre-edge region, however, there is good agreement, with the computed spectra showing a suppression of the pre-edge feature upon CO₂ adsorption. When mmen is appended to the Mg sites, the pre-edge region splits into two low-intensity features, much like DMF-ligated Mg-MOF-74, but there is greater intensity in the higher-energy feature, in agreement with the general spectral shape seen in experiment.

By analyzing the excited electronic states associated with the computed transitions for Mg₂(dobpdc), we observe analogous behavior to Mg-MOF-74, but the situation is complicated by greater hybridization with the π system of the longer organic linkers. This results in many low-intensity transitions to π states on the linkers that only weakly mix with the distorted lobe at the Mg center. The most intense transitions, however, are similar to those seen in Mg-MOF-74. The intensity of the pre-edge feature for activated Mg₂(dobpdc) arises primarily from two transitions, with roughly equal intensity. These excited states for these transitions both feature the same localized, distorted lobe seen for Mg-MOF-74, but both show significant hybridization

with the π system on the linkers, reducing the transition intensities due to delocalization. The wavefunction for the higher-energy state is shown in Figure S7a, and is analogous to Mg-MOF-74. The CO₂ and mmen cases are analogous to CO₂ and DMF in Mg-MOF-74, as can be seen from the wavefunctions shown in Figure S7b and S8c. CO₂ shows hybridization with the distorted lobe at the Mg site, lowering the transition intensity primarily through delocalization, while mmen lowers the transition intensity by partially restoring spherical symmetry at the Mg site. It should be noted that static and dynamic disorder of the amines is not considered here, and may play a role in the electronic structure of the real system.

Figures:

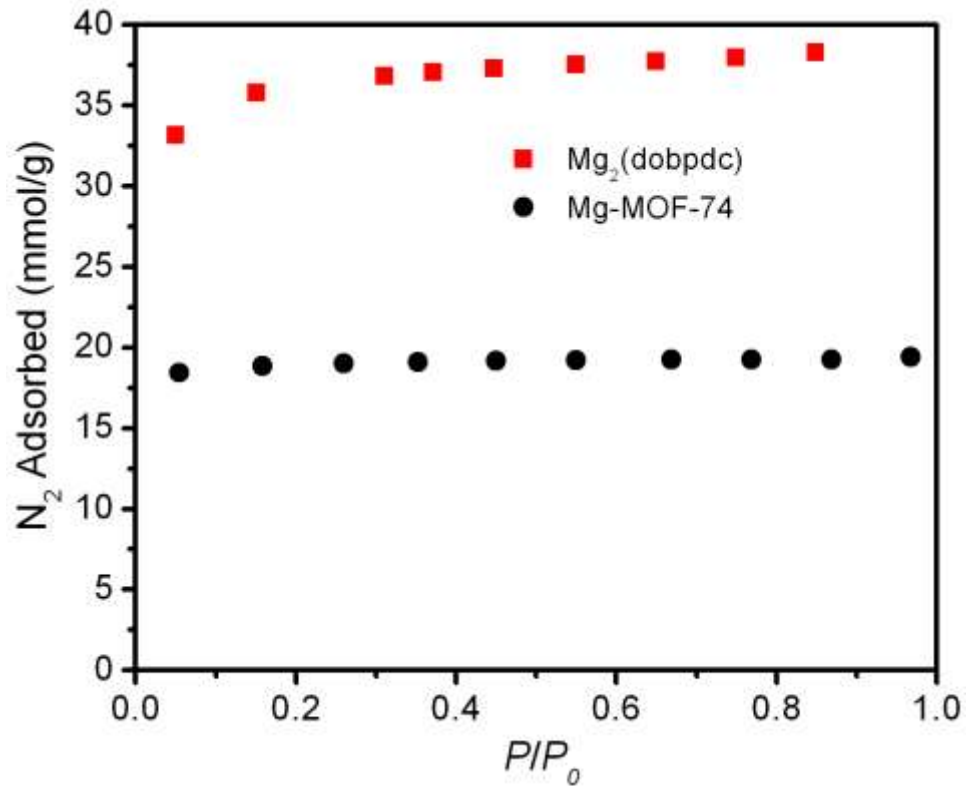


Figure S1: Adsorption of N₂ at 77 K for activated Mg-MOF-74 (black) and Mg₂(dobpdc) prior to transmission sample deposition.

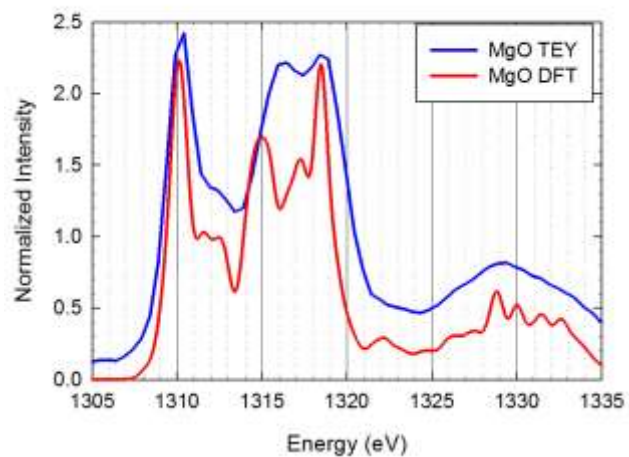


Figure S2: Total electron yield (TEY) spectrum of the Mg K-edge of cubic MgO, and the same spectrum calculated from DFT. Both spectra were aligned to previous data from Lindner et al. (see text). The experimental spectrum was used for absolute energy calibration of all NEXAFS spectra collected at the Mg K-edge. Similarly, the theoretical spectrum was used to calibrate the energy of all computed NEXAFS spectra in this study.

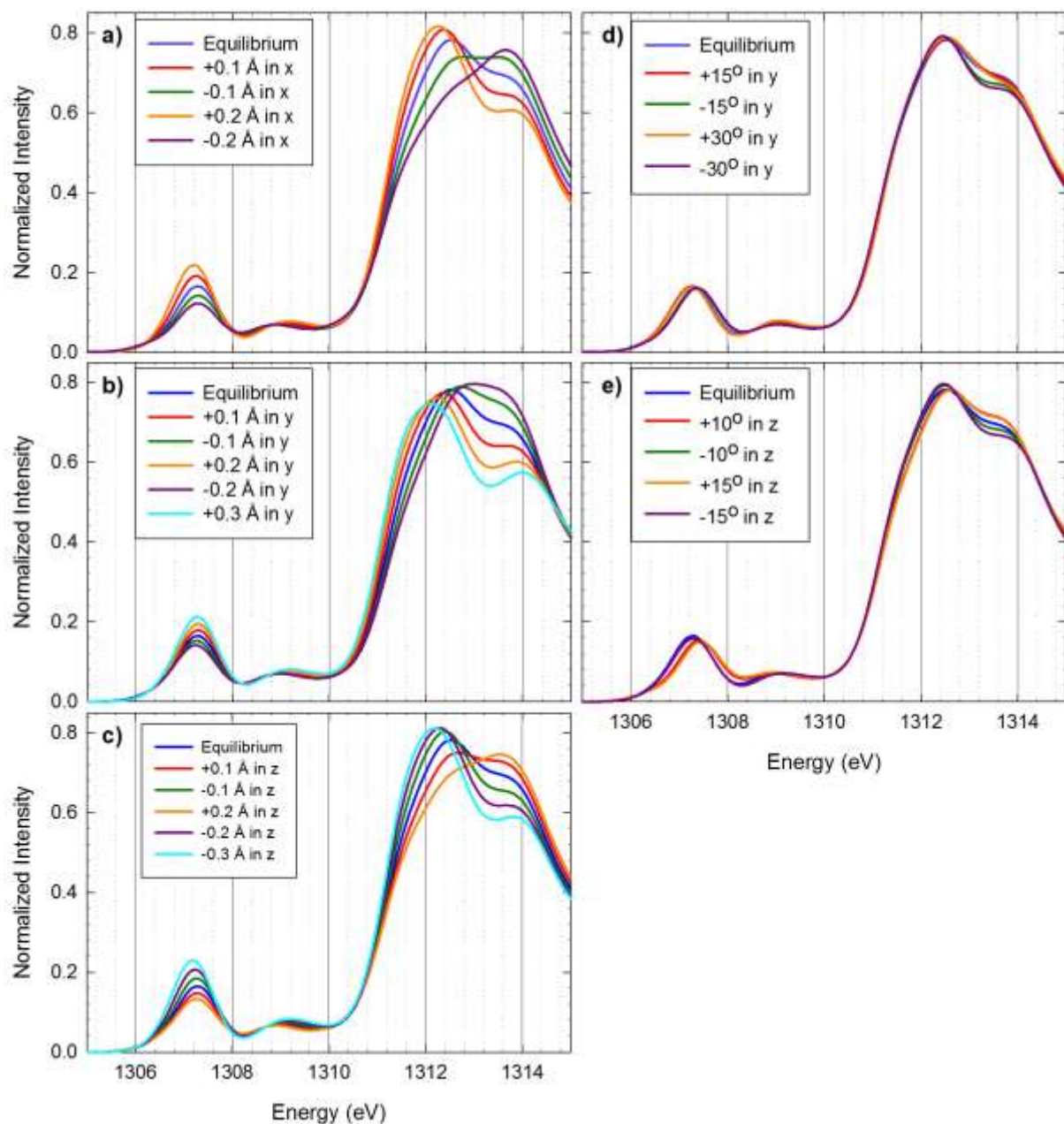


Figure S3: Computed Mg *K*-edge NEXAFS spectra for Mg-MOF-74 with adsorbed CO₂, as a function of **a)** CO₂ translation in x, **b)** CO₂ translation in y, **c)** CO₂ translation in z, **d)** CO₂ rotation in y, and **e)** CO₂ rotation in z. Translations and rotations are computed around the equilibrium positions. Rotations are performed around the O atom of the CO₂ that is coordinated to the Mg center. The translations and rotations shown result in a total energy change

compatible with room temperature; however, the Boltzmann-weighted average of these motions generates a spectrum that is indistinguishable from the equilibrium spectrum. This implies that thermal motion of the framework has a larger impact on the NEXAFS spectrum than thermal motion of the adsorbed CO₂.

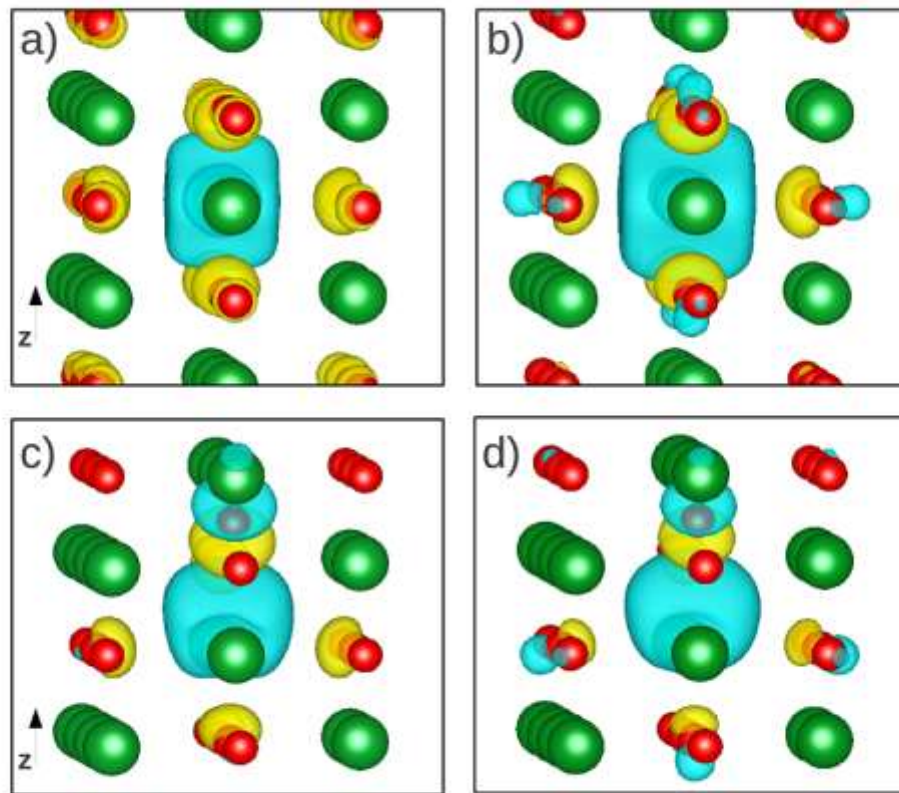


Figure S4: Upper panels: wavefunctions corresponding to the lowest-energy state (panel a) and second lowest-energy state (panel b) for MgO from the excited electron and core hole calculation. Lower panels: wavefunctions corresponding to the lowest energy state (panel c) and second lowest energy state (panel d) for MgO in which the apical oxygen bond length has been increased by 0.5 Å.

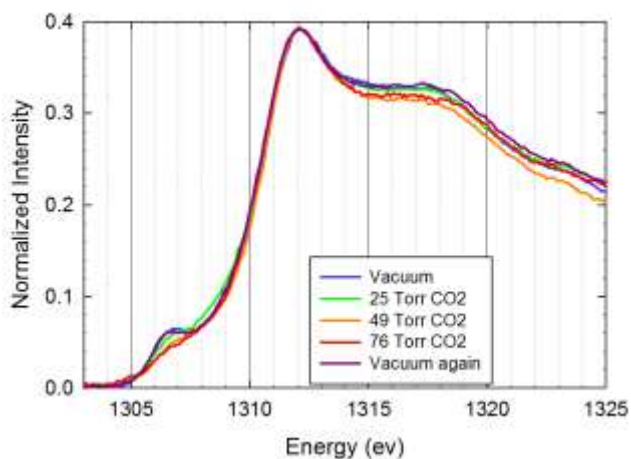


Figure S5: Mg K-edge NEXAFS spectra of Mg₂(dobpdc) in vacuum, with CO₂ gas pressures of 25 Torr, 49 Torr, and 76 Torr, corresponding to 0.52, 0.65 and 0.72 CO₂ molecules per Mg site, respectively, and in vacuum again following gas exposure. Spectra were subjected to a linear baseline correction, but were normalized to the main edge intensity due to complications from time-dependent drift in the intensity. The pre-edge region shows a distinct change upon CO₂ adsorption like that seen for Mg-MOF-74, which reverses when the gas is pumped out.

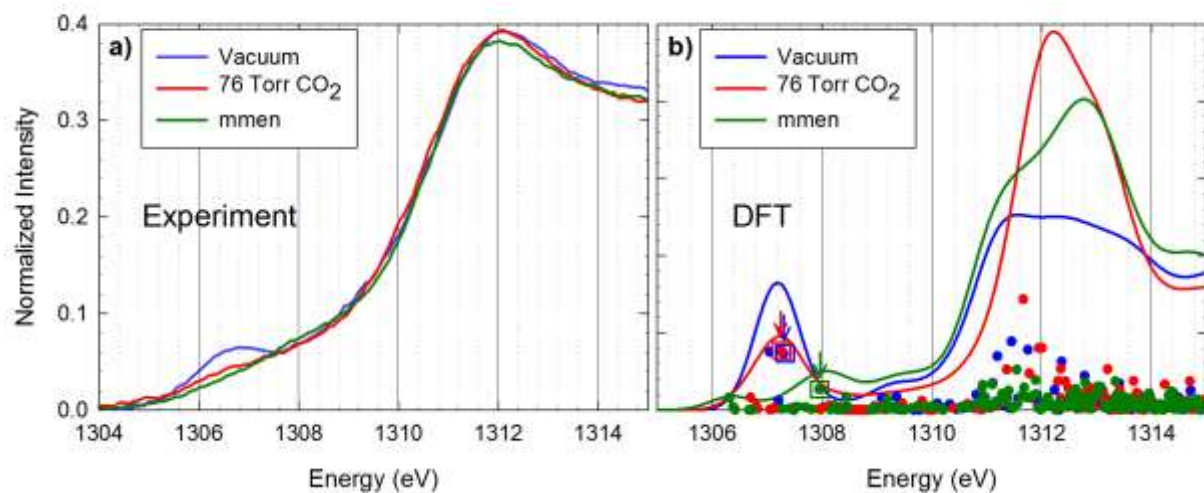


Figure S6: a) NEXAFS spectra for activated $\text{Mg}_2(\text{dobpdc})$ (blue), $\text{Mg}_2(\text{dobpdc})$ with 76 Torr CO_2 (red), and $\text{Mg}_2(\text{dobpdc})$ with mmen appended to the Mg sites (green). These data are normalized to the main edge intensity due to time-dependent intensity drift. **b)** Calculated NEXAFS spectra (lines) for activated $\text{Mg}_2(\text{dobpdc})$ (blue), $\text{Mg}_2(\text{dobpdc})$ with adsorbed CO_2 (red) and $\text{Mg}_2(\text{dobpdc})$ with mmen appended to the Mg sites (green), along with transition probabilities (circles) from which the spectra were generated. The transitions with the largest contribution to the pre-edge intensity are marked with a colored square and arrow.

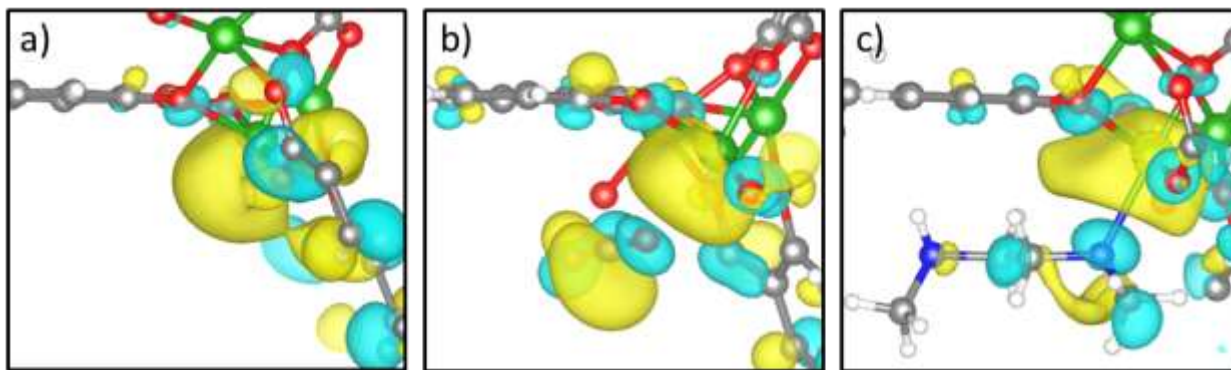


Figure S7: **a)** The excited state wavefunction corresponding to the blue marked transition in Figure S6. Mg atoms are shown in green, oxygen atoms in red, carbon atoms in grey and hydrogen atoms in white. The two phases of the wavefunction are shown in yellow and teal. **b)** The excited state wavefunction corresponding to the red marked transition in Figure S6. **c)** The excited state wavefunction corresponding to the green marked transition in Figure S6. Colors are the same as previous panels, with the addition of nitrogen atoms shown in blue.

References:

- (1) Britt, D.; Furukawa, H.; Wang, B.; Glover, T. G.; Yaghi, O. M. *Proceedings of the National Academy of Sciences of the United States of America* **2009**, *106*, 20637.
- (2) McDonald, T. M.; Lee, W. R.; Mason, J. A.; Wiers, B. M.; Hong, C. S.; Long, J. R. *Journal of the American Chemical Society* **2012**, *134*, 7056.